Vol. 41, No. 4 (2019) 563-572, DOI: 10.24874/ti.2019.41.04.09

Tribology in Industry

www.tribology.rs

RESEARCH

Mechanical and Tribological Analysis of Anodized AZ31 Magnesium Alloy as a Function of a Cement Concrete Environment

J.C. Caicedo[a,*], S. Quiñonez[a], W. Aperador[b]

[a] *Tribology, Polymers, Powder Metallurgy and Processing of Solid Recycled Research Group, Universidad del Valle, Cali, Colombia,*
[b] *School of Engineering, Universidad Militar Nueva Granada, Bogotá, Colombia.*

Keywords:

AZ31 alloy
Anodized MgO
Mechanical properties
Friction coefficient
Ceramic concrete

* Corresponding author:

Julio Cesar Caicedo Angulo
E-mail:
julio.cesar.caicedo@correounivalle.edu.co

Received: 19 June 2019
Revised: 25 July 2019
Accepted: 18 September 2019

A B S T R A C T

Anodized AZ31 Magnesium Alloys was synthesized via electrodeposition processes. The aim of this work was to determine the mechanical and tribological response of the anodized AZ31 Magnesium alloy with different current densities immersed under cement concrete paste with different solidification times. The samples of the anodized alloy were characterized by microindentation so, the mechanical properties (micro-hardness) was increased by 32 % when the magnesium alloy was anodized with a current density of 25 mA/cm², in this sense the friction coefficient between the anodized AZ31 magnesium (MgO) obtained with the highest current density and the metallic AZ31 alloy exhibited a reduction of 54.5 %. The scratch test and wear rate (abrasive sliding of cement concrete) show an increase in the critical load and a reduction of weight loss as a function of the applied current density around of 49 % and 92.3 %, respectively. Scanning electron microscopy was performed to analyze morphological surface changes on the anodized AZ31 alloy after tribological tests. The tribological behavior of the anodized AZ31/MgO system indicates that the AZ31/MgO coatings can have a promising future in applications for the civil construction industry.

1. INTRODUCTION

Every day the construction of civil works demands more novel processes that allow meeting the high demand applications in the construction industry. Therefore, civil structures based on cement set require procedures that guarantee a fast pouring and drying, which implies that the cement set (concrete ceramic) contain additives such as super plasticizers that help the rapid solidification. Furthermore, the devices that allow to give an established geometrical shape to the cement in its fresh state or scaffold must also have characteristics that allow a fast solidification of the concrete and an easy demolding to obtain the solidified structure [1,2]. Taking into account the

above, the magnesium scaffold (forms) arise as an alternative that meets the requirements in the demolding process; however, they are wear and adhesion problems between the magnesium scaffold and the solidified, hardened concrete [3,4]. In this sense the tribological wear in magnesium forms presents a problem in the industrial sector due to its high use in the civil constructions works. Moreover, various authors have reported the abrasive and adhesive wear suffered by magnesium alloys under various conditions such as casting alloys and molds for concrete hardening [5,6]. Taking into account the above, when the wear effect is severe it reduces the industrial applications, therefore, the need arises to apply a treatment on the magnesium alloy's surface to increase the ranges of application, then the anodizing processes have been an alternative for improving the properties of AZ31 alloys. Thus, the anodizing process result produces, among other effects, a MgO layer which, due to its the ceramic nature, cooperates in the wear resistance by generating severe slip, thus reducing the excessive wear rates [7,8]. To obtain the stable, resistant and durable MgO layer, the variables in the anodizing process are fundamental; consequently, the current densities, the immersion time, and the type of alkaline solution can modify the thickness, the mechanical properties, wear and corrosion resistance when the AZ31/MgO system is exposed in aggressive environments under corrosive solutions and under products obtained by ceramic concrete solidification [9-11]. However, in scientific literature few studies have focused on the anodized Mg (AZ31) alloy and its interaction with solidified cement concrete (ceramic paste). Therefore, this research studied anodized MgO coatings which were obtained on metallic AZ31substrates using different current densities for the anodizing process. The AZ31/MgO system was analyzed under abrasive wear conditions through the wear in inclined plane, by sliding the fresh concrete (ceramic paste) onto the anodized alloy surface in order to determine its possible applications for the civil construction industry.

2. METHODS AND MATERIALS

AZ31 magnesium alloy samples were deposited into a square area of 2 mm^2, and the working surface was submerged in electrolyte (1 mm^2); moreover, the samples were polished with abrasive papers, followed by emerging them in isopropyl alcohol. All anodizing experiments were performed in 250 mL of modified Harry Evangelides (HAE) solution which contained KOH (132 g/L), $Al(OH)_3$ (27.2 g/L), K_2F_2 (27.2 g/L), Na_3PO_4 (27.2 g/L), and $KMnO_4$ (15.2 g/L) [12]. The anodizing processes were carried out at current density values of 15, 20 and 25 mA/cm^2, performed at 30°C in 60 min. Morphological surface properties in the anodized magnesium were studied by scanning electron microcopy (SEM) using a JSM 6490LV JEOL. The mechanicals properties (Vickers hardness) were carried out by using a microindenter, (ZWICK Roell Indectec) with a pyramid-shaped diamond tip and a base angle of 136°. A constant load of 0.2 kg was applied and a holding time of 20 seconds to observe the indentation trace by means of a microscope with a 400X magnification; the average of the diagonals of the square footprint was determined to perform the hardness calculation in agreement with ASTM E384 [13]. Tribological characterization was done by means of a Microtest, MT 400-98 tribometer, using an alumina (Al_2O_3) ball with 6 mm in diameter as a pin in order to make reference to the fact that the tribological pair corresponds to surfaces of a ceramic nature. The applied load was 0.5 N with a total running length of 800 m. The layer's adherence was studied by using a Scratch Test Microtest MTR2 system, applying a scratch length of 6 mm and a raising load of 0 N –60 N. The ceramic paste formulation was made taking into account the optimal water - cement ratio and the dosage used to make the ceramic paste (mortar) for the mechanical tests are presented in Table 1.

Table 1. Dosing of the ceramic paste (concrete cement or mortar) used in the tensile tests to determine the adhesive behavior between the AZ31 alloy and the cement concrete.

Specification for ceramic paste design	Value	ASTM (Ref.)
Water/cement ratio	0.67	C-187-86 [14]
Aggregate/cement ratio	3	
Cement	32.8 g/cm^3	
Accelerator (% cement weight)	1%	
Sand granulometry		
Maximum nominal size	2.4 mm	C-136:2005 [15]
Type of sand	Angular	
Fineness module	2.61	
Features fresh (ceramic paste)		
Fluency	115	C-230-90 [16]
Mechanical properties (ceramic paste)		
Mechanical resistance (7 days)	16.96 MPa	C-230-90 [16]
Mechanical resistance (28 days)	22 MPa	

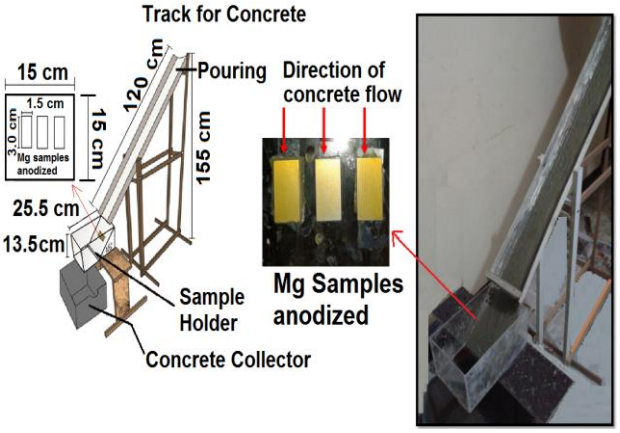

(a) (b)

Fig. 1. Experimental assembly of the wear simulation of anodized AZ31 alloy at different current densities with fresh concrete. (a) design scheme used in wear simulation and (b) wear in inclined field photography.

The wear by sliding on an inclined plane of fresh concrete was carried out with the aim of performing a test that simulates the anodized magnesium application, where wear occurs when fresh concrete slides on the surface of anodized samples obtained at different current densities [17]. This experimental setup is showed in the Fig. 1. From this test, the mass loss suffered by the different types of samples under 100 cycles of sliding concrete was measured by gravimetry, which has a fresh bulk density of 2.04 ± 0.01 g/ml in room temperature (~25 °C). The experimental assembly includes a track for concrete pouring, a sample holder and a concrete collector.

3. RESULTS

3.1 Mechanicals properties

From microindentation measurements, the Vickers micro-hardness values for the AZ31 alloy substrate and the different anodized alloys were obtained, in agreement with ASTM E384 standard [13]. In Fig. 2, the optical microscopy shows the micrographs for indentation traces which were taken at 50X. It is noticeable that the indentation trace's size was reduced when the AZ31 alloy was set to the superficial anodizing process. Therefore, when the current density increased in the anodizing process to form the ceramic MgO layer, an increase in layer density occurred, as was analyzed from the SEM results showed in the previous work [18]; thus, a reduction in the indentation trace size was observed in the AZ31/MgO system obtained with the highest current density.

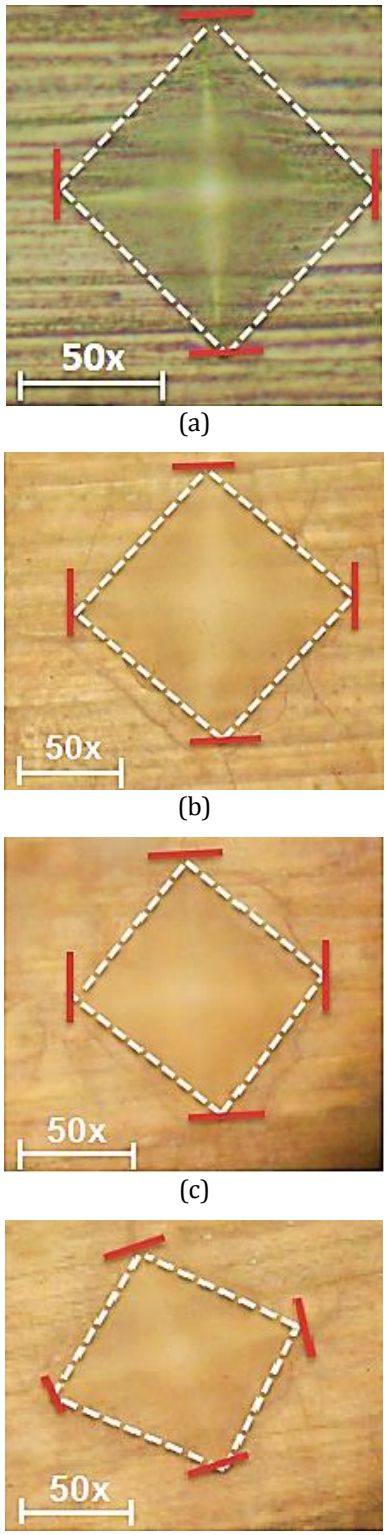

(a)
(b)
(c)
(d)

Fig. 2. Optical micrographs of microindentation traces taken at 50X by Caicedo et al. in 2019 [18]: (a) Mg metal alloy (AZ31), (b) metal alloy (AZ31) anodized (MgO) with 15 mA/cm^2, (c) MgO anodized with 20 mA/cm^2 and (d) MgO anodized with 25 mA/cm^2.

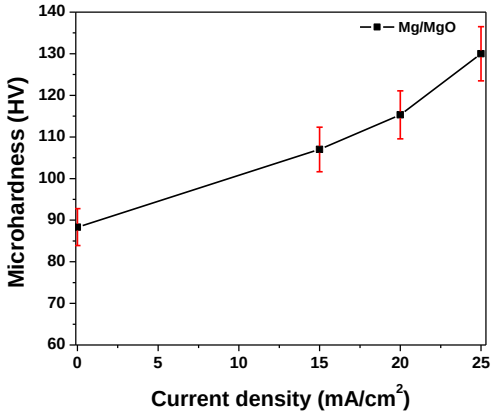

Fig. 3. Surface micro-hardness behavior from the Mg alloy and MgO as a function of the anodizing current density by Caicedo et al. in 2019 [18].

Figure 3 shows the increase in micro-hardness as a function of the anodizing current density, where it is possible to analyze that an increasing current density in the anodizing process increases the micro-hardness of the AZ31/MgO system in relation to the metallic Mg-alloy substrate (AZ31). In this sense, the interacting mechanisms between the metallic AZ31 alloy and ceramic AZ31/MgO with high density produced a mechanical adjustment that restricted the propagation of deformation energy when the load was applied [19]. Furthermore, the grain size reduction by the MgO densification observed from the SEM results [18] contributed in generating an increase in hardness as a function of the current density increasing.

3.2 Tribological properties

3.2. 1 Pin on disc test

Figure 4 shows the friction coefficient as a function of the sliding distance for the metallic AZ31 Mg alloy (substrate) and the different anodized alloys, varying the current density from 15, 20 to 25 mA/cm2. All of the curves showed two typical stages: stage I, where the friction coefficient increased to a high value, and stage II, where there was a decay of the friction coefficient to a stabilizing zone. The friction coefficient increase is attributed to the period of time which gives a strong interaction between the two rough surfaces on the tribological pair, leading to the detachment of particles which are generated by surface wear [20]. Therefore, stage II is known as the stable zone or sliding distance. Once the roughness of both surfaces is smoothed, the surface of the less hard material, in this case the coated system AZ31/MgO (AZ31 anodized), is molded to the surface of the harder material (alumina pin), thus reducing the friction coefficient until the start of the steady state [21, 22]. Figure 4b shows the friction coefficient variation as a function of the anodizing current density. In this case, a reduction in the friction coefficient is observed when the current density increases. This is related to the frictional model proposed by Archard (Eq. 1) which contemplates the surface roughness contribution, the pin nature and the coating hardness [23].

$$\mu = C_k \frac{R_{(s,a)}}{\sigma_{t(H,E)}} \tag{1}$$

where μ is the friction coefficient of the tribological pair, C_k is an adjustment constant that depends on the test conditions, $R_{(s,\,a)}$ is the coating roughness, $\sigma_{t(H,\,E)}$ is a variable that depends on the mechanical properties of the system (hardness H or elasticity modulus E).

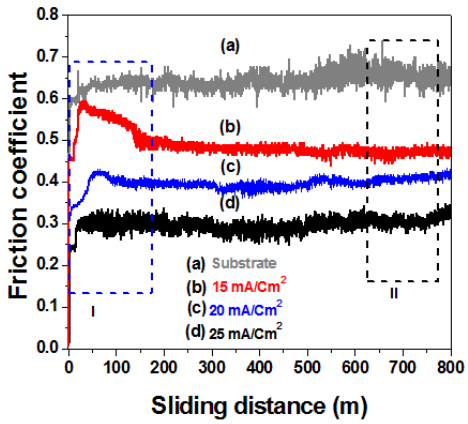

(a)

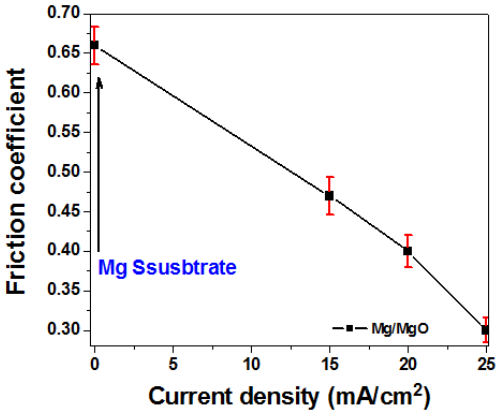

(b)

Fig. 4. Tribological tests for the non-anodized and anodized magnesium alloy AZ31/MgO: (a) friction coefficient as a function of the sliding distance, (b) friction coefficient reduction as a function of the anodizing current density by Caicedo et al. in 2019 [18].

Figure 5 shows the SEM micrographs for the wear tracks obtained for the anodized AZ31 alloys with different current densities, which evidence the abrasive wear produced by the continuous passage of the (Al_2O_3) pin on the AZ31/MgO surface, generating micro-fractures. So, the micro-fractures when are detached from the substrate form wear tracks in the surface material. For the anodized alloys, a recombination of the metal surface can be evidenced with the MgO coating caused by abrasive wear. When the current density increased in the anodizing process, the mechanical properties increased, and the friction coefficient as well as the width of the wear track decreased. The wear reduction indicates that the MgO densification reduced the severe wear which is attributed to the fact that the anodized AZ31 alloy with a current density of 25 mA/cm^2 supported the weight of the load and the friction generated by the sliding of the ceramic alumina pin on the AZ31 surface.

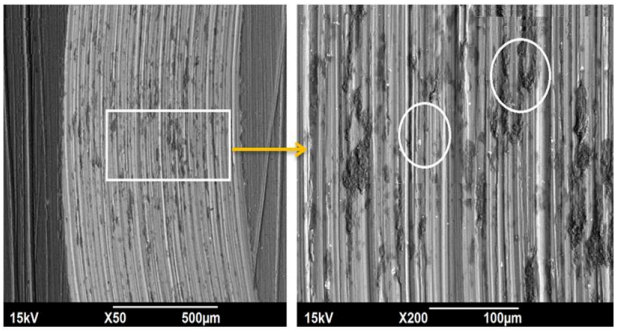

(a)

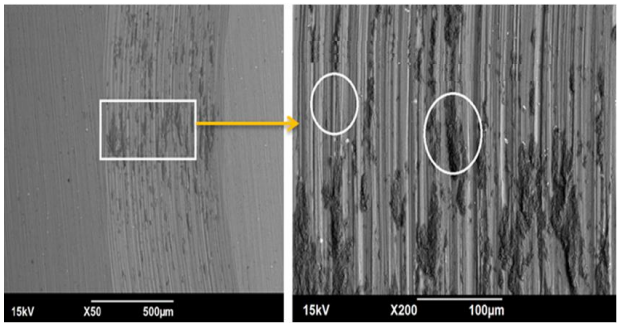

(b)

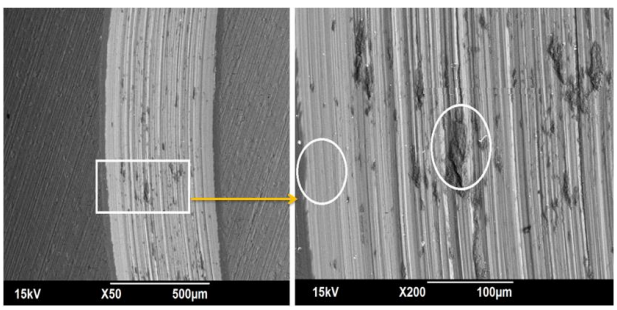

(c)

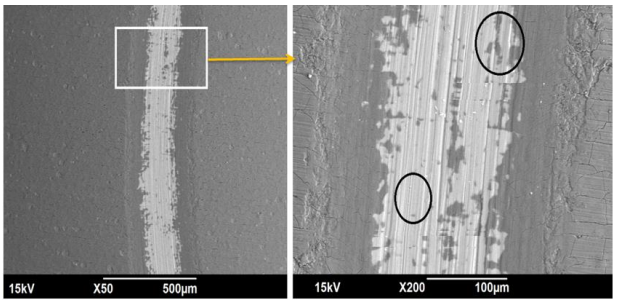

(d)

Fig. 5. SEM micrograph of the wear track: (a) metallic AZ31 alloy, (b) anodized AZ31 alloy with 15 mA/cm^2, (c) anodized AZ31 alloy with 20 mA/cm^2 and (d) anodized AZ31 alloy with 25 mA/cm^2.

According to the Archard model described above, when the MgO coating (anodized AZ31 alloy) has high hardness the friction coefficient tends to decrease, which is related to the micro-hardness results (Fig. 5). Therefore, by increasing the current density of the anodizing process, the friction coefficient shows lower values. For the anodized AZ31 alloy with greater hardness, which was obtained with a current density of 25 mA/cm^2, the friction coefficient decreased around 54.5 % with respect to the non-anodized (AZ31) magnesium alloy or without MgO coating (substrate).

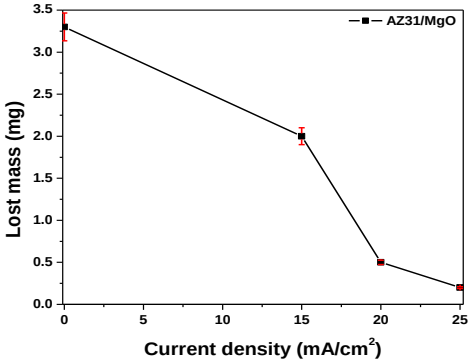

Fig. 6. Mass loss behavior in the pin on disk test as a function of the current density in the anodizing process.

Taking into account the above, the wear resistance was determined from the friction test results, when the AZ31/MgO system was subjected to a sliding distance of 800 m and taking as reference the weight loss value. By analyzing the wear tracks from the SEM micrographs, it was possible to identify the wear phenomena that were presented on the surface when there was a severe break in the continuity of the MgO coating. In Fig. 6 it is possible to see the mass loss presented by the AZ31/MgO

system in the friction test (pin on disk) as a function of the current density. Moreover, it is possible to analyze that the weight loss is lower for the MgO coating obtained with higher current density due to the increase in coating thickness and hardness of the anodized alloys).

3.2.2 Scratch Test

From the scratch test, the adhesion strength of the anodized MgO coating was characterized taking into account two terms: the critical load LC_1, which is defined as the load where the first cracks occur (cohesive failure); and the upper critical load LC_2, where the delamination occurs at the edge of the scratch track (adhesive failure) [21,22]. Many authors have tried to find an expression that relates different variables that are present in the scratch test, such as Holmberg, who has proposed one model where the friction between the layer and the scratch indenter and the mechanical properties of the layer are taken into account [24].

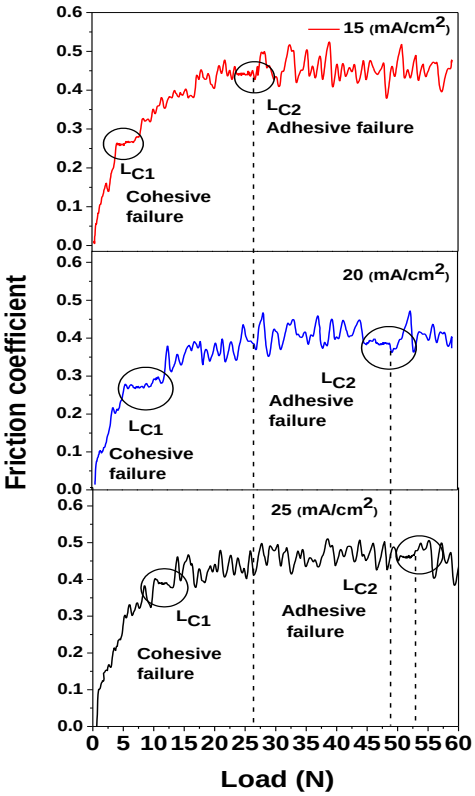

Fig. 7. Friction coefficient curves as a function of the applied load for the anodized magnesium alloy AZ31 anodized at different current densities exhibiting the cohesive failure (LC_1) and adhesive failure (LC_2).

Figure 7 shows the critical load values for the anodized Mg/MgO system at different current densities. In Fig. 7 both loads are shown, where the dotted line indicates the critical load LC_2. The different critical loads were determined from the area where the load becomes more independent of the friction coefficient. The first stabilization of the curve is attributed to the cohesive failure, while the second stabilization is attributed to the adhesive failure.

In Fig. 8 it is possible to observe the critical load behavior when the current density was varied in the anodizing processes. The increase of the critical adhesive load of around 49% is due to the increase of the mechanical properties, as well as the reduction of the surface roughness and the friction coefficient reduction. From this behavior it is analyzed that the mechanical properties (hardness) generated by the densification of the anodizing processes act as a block to the propagation of cracks, because of this the anodized AZ31 alloy (MgO) with high current densities supports greater loads preventing the coating delamination (adhesive failure) [25].

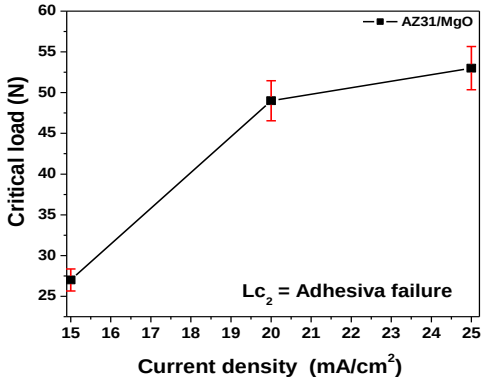

Fig. 8. Critical load curves as a function of the current density in the anodizing processes for magnesium AZ31 alloy.

Figure 9 shows the SEM micrographs taken of the wear tracks of the magnesium AZ31 alloys' surface anodized at different current densities, where it is possible to distinguish the zones where the different critical loads generated the different failure types such as cohesive (LC_1) and adhesive (LC_2) failure. So, when the current density increased for the anodizing processes associated to 25 mA/cm^2, the critical load value increased, so, the surface damage reduction was lower in relation to the other current densities; therefore, this phenomenon was attributed to the densification increase, the coating thickness variation and the mechanical properties increase.

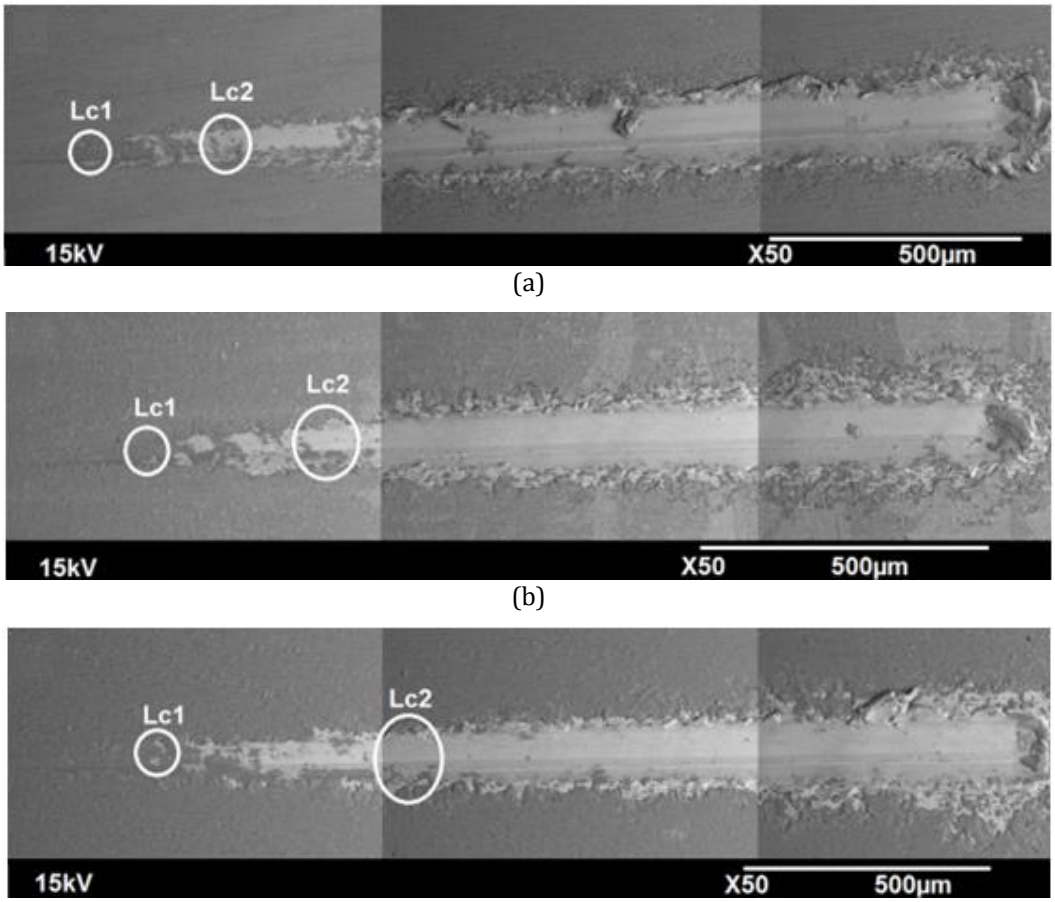

Fig. 9. Scanning electron microscopy of the wear track generated by the scratch test for the anodized magnesium AZ31 alloy: (a) 15 mA/cm^2, (b) 20 mA/cm^{2}and (c) 25 mA/cm^2.

3.2.3 Wear in inclined plane

The wear in inclined plane for the anodized magnesium AZ31 alloy with different current densities under ceramic paste (concrete material) sliding was carried out with the experimental assembly taking into account the fluid speed, the concrete mixture properties and the sand granulometry (Fig. 1). Through the SEM micrographs and EDX, results were obtained to identify the wear produced on the anodized AZ31 alloys' surface by passing the fresh concrete 100 times over the AZ31 alloys and obtaining the chemical composition of the products generated on the wear surface.

Figure 10 shows the micrographs obtained for the Mg AZ31 alloy without the anodizing process (substrate) and the anodized alloys (MgO coatings) obtained with different current densities. So, the abrasive wear can be observed in the micrographs, which shows reduction when the anodizing current density is increased. The reduction of wear phenomenon can be attributed to the increase in the mechanical properties of the coating (MgO). Therefore, it was possible to analyze that the non-anodized AZ31 alloy (substrate) present a surface cracking phenomena due to the material detachment generated by the intense abrasion associated with the low mechanical properties (metallic alloy). Moreover, the concrete material (ceramic paste) had Cl^- ions that were found in the ceramic mixture and this generated pitting corrosion on the alloy since it did not have MgO material as a protection layer [26,27].

On the contrary to the non-anodized AZ31 alloy (substrate), in the anodized alloys with different current densities it is shown that there was little detachment of the coating surface, evidenced by areas with changes in the gray scale, and in that sense less detachment can be observed when the current density in the anodizing processes was increased. Finally, the concrete material adhesion on the anodized alloy surface like incrustations can also be evidenced, and the adherence is less evident as the current density increased in the anodizing process [28].

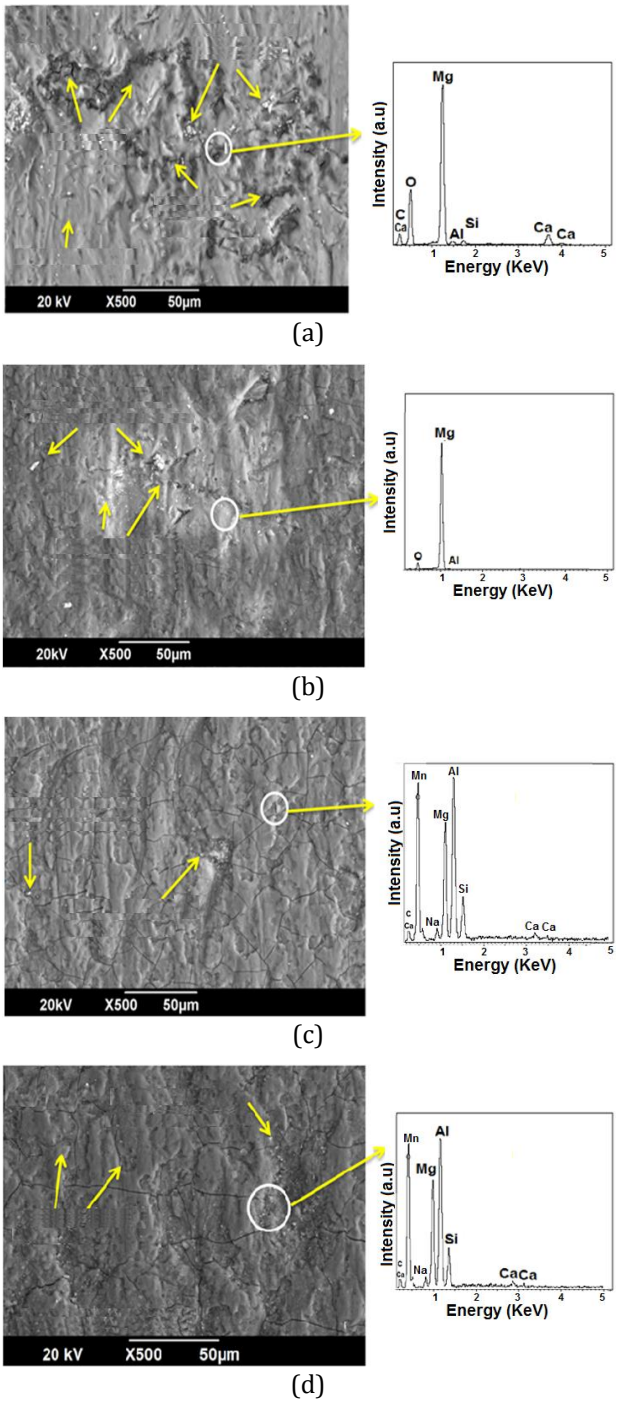

Fig. 10. SEM-EDX micrograph of the wear surface showing the abrasion produced after 100 sliding cycles in the inclined plane of fresh concrete: (a) metal alloy (AZ31), (b) anodized metal alloy AZ31/MgO with 15 mA/cm², (c) anodized AZ31/MgO alloy with 20 mA/cm² and (d) anodized AZ31/MgO alloy with 25 mA/cm².

3.2.4 Mass Loss Analysis by Sliding on inclined plane

In order to evaluate the wear rate on the non-anodized (substrate) and the anodized AZ31 alloy (AZ31/MgO coating) surface under the different cycles in the inclined plane sliding of fresh concrete (ceramic paste), the mass loss analysis was carried out.

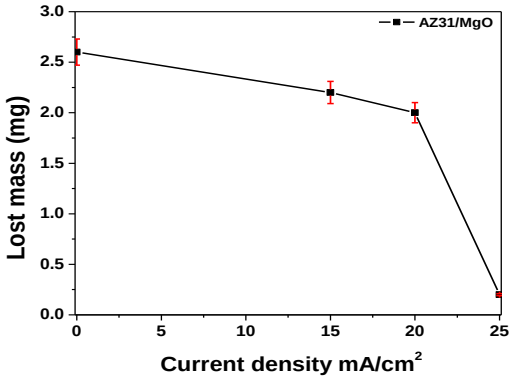

Fig. 11. Wear rate analyzed by mass loss in the non-anodized and anodized AZ31 alloy with different current densities under fresh concrete applied by sliding in an inclined plane.

Figure 11 shows the mass loss as a function of the current density in the anodizing process, where it is clearly shown that the sliding concrete generates material loss [28-30]. Taking into account that the abrasive wear mechanism produces surface reduction, a mass loss reduction of around 92.3 % can be evidenced when the AZ31 alloy was anodized with the highest current density value. This reduction can be attributed to the coating thickness and the surface hardness increase by the anodizing processes with the current density applied. Additionally, a mass lost reduction in the pin-on-disk test was also observed, with the friction coefficient reduction (Fig. 4) as a function of the current density increasing, which generates the wear resistance improvement and opening thus the possibility of future applications in the civil constructions field.

4. CONCLUSION

Microindentation results show the increasing for micro-hardness of around 32% due to the densification effect when the current density in the anodizing processes for AZ31/MgO alloy was increased from 15 mA/cm² to with 25 mA/cm².

From the pin-on-disk analysis, a reduction in friction coefficient of around 54.5% was observed when the current density in the anodizing processes was increased, so it can be concluded that when the anodized AZ31 alloy (AZ31/MgO)

presented high density and higher surface hardness, the friction coefficient tended to decrease, which evidence greater wear resistance.

From the scratch and the wear rate analysis by sliding fresh concrete in inclined plane on the AZ31/MgO system, an increase in the load for adhesive failure and a decrease in the wear rate could be observed for the anodized substrates when the current density in the anodizing process increased. This increase in the load favors the MgO coating adhesion on the AZ31 alloy, reducing thus the wear associated to the mechanical properties increase and the friction coefficient reduction, evidencing longer useful life for the AZ31 alloy when it is used in metal forms applications.

Acknowledgement

This study has been supported by the Vicerrectoría de Investigaciones de la Universidad Militar Nueva Granada with project number ING-2992, validity 2019.

REFERENCES

[1] I. Man-Chi Lo, C.I. Tang, X. D. Li, C.S. Poon, *Leaching and Microstructural Analysis of Cement-Based Solidified Wastes,* Environmental Science & Technology, vol. 34, iss. 23, pp. 5038–5042, 2000, doi: 10.1021/es991224o

[2] D. Jinfeng, H. Guangsheng, Z. Yanchun, W. Bei, *Electrochemical Performance of AZ31 Magnesium Alloy under Different Processing Conditions*, Rare Metal Materials and Engineering, vol. 43, iss. 2, pp. 316–321, 2014, doi: 10.1016/S1875-5372(14)60066-7

[3] Liyuan. Chai, Xia. Yu, Zhihui. Yang, Yunyan. Wang, Masazumi Okido, *Anodizing of magnesium alloy AZ31 in alkaline solutions with silicate under continuous sparking*, Corrosion Science, vol. 50, iss. 12, pp. 3274-3279, 2008, doi: 10.1016/j.corsci.2008.08.038

[4] C.S. Wu, Z. Zhang, F.H. Cao, L.J. Zhang, J.Q. Zhang, C.N. Cao, *Study on the anodizing of AZ31 magnesium alloys in alkaline borate solutions*, Applied Surface Science, vol. 253, iss. 8, pp. 3893-3898, 2007, doi: 10.1016/j.apsusc.2006.08.020

[5] L.A. Dobrzański, T. Tański, L. Čížek, J. Domagał, *Mechanical properties and wear resistance of magnesium casting alloys*, Journal of Achievements in Materials and Manufacturing Engineering, vol. 31, iss. 1, pp. 83-90, 2008.

[6] N.N. Aung, W. Zhou, L.E.N. Lim, *Wear behaviour of AZ91D alloy at low sliding speeds*, Wear, vol. 265, iss. 5-6, pp. 780-786, 2008, doi: 10.1016/j.wear.2008.01.012

[7] Y. Fouad, M. El Batanouny, *Effect of surface treatment on wear behavior of magnesium alloy AZ31,* Alexandria Engineering Journal, vol. 50, iss. 1, pp. 19-22, 2011, doi: 10.1016/j.aej.2011.01.003

[8] C. Liang, X. Han, T. F. Su, C. Li, J. An, *Sliding Wear Map for AZ31 Magnesium Alloy*, Tribology Transactions, vol. 57, iss. 6, pp. 1077-1085, 2014, doi: 10.1080/10402004.2014.933939

[9] T. Sugita, H. Yasunaga, *Friction and wear of MgO single crystals on sintered Al2O3 in vacuum*, Wear, vol. 40, iss. 1, pp. 121-128, 1976, doi: 10.1016/0043-1648(76)90023-5

[10] H. Ye, X. B. Zhang, X. Chang, R. Chen, *Microstructures and Properties of Laser Al Alloying on AZ31 Magnesium Alloy*, Advanced Materials Research, vol. 189-193, pp. 867-870, 2011, doi: 10.4028/www.scientific.net/AMR.189-193.867

[11] Y. Mizutani, S.J. Kim, R. Ichino, M. Okido, *Anodizing of Mg alloys in alkaline solutions*, Surface and Coatings Technology, vol. 169–170, pp. 143-146, 2003, doi.org/10.1016/S0257-8972(03)00214-7

[12] C. Blawert, W. Dietzel, E. Ghali, G. Song, *Anodizing Treatments for Magnesium Alloys and Their Effect on Corrosion Resistance in Various Environments*, Advanced Engineering Materials, vol. 8, iss. 6, pp. 511–533, 2006, doi: 10.1002/adem.200500257

[13] ASTM E384-17 *Standard Test Method for Microindentation Hardness of Materials,* 2017, doi: 10.1520/E0384-17

[14] ASTM C 187-86. *Standard Test Method for Normal Consistency of Hidraulic Cement. Philadelphia*, 1990, doi: 10.1520/E0187-86

[15] ASTM C 136-05. *Standard Test Method for Sieve Analysis of Fine and Coarse Aggregates Philadelphia*, 2005, doi: 10.1520/E0136-05

[16] ASTM C-230-90. *Standard Specification for Flow Table for Use in Tests of Hydraulic Cement. Philadelphia,* 1990, doi: 10.1520/E0230-90

[17] L. Yu, J. Cao, Y. Cheng, *An improvement of the wear and corrosion resistances of AZ31 magnesium alloy by plasma electrolytic oxidation in a silicate–hexametaphosphate electrolyte with the suspension of SiC nanoparticles,* Surface and

Coatings Technology, vol. 276, pp. 266-278, 2015, doi: 10.1016/j.surfcoat.2015.07.014

[18] J.C. Caicedo, F. Franco, W. Aperador, *Variation of adhesive stress in anodized AZ31 magnesium alloy immersed within cement concrete blocks with different solidification times*, Materials Chemistry and Physics, vol. 232, pp. 414–421, 2019, doi: 10.1016/j.matchemphys.2019.05.015

[19] D. Zhang, Y. Gou, Y. Liu, X. Guo, *A composite anodizing coating containing superfine Al2O3 particles on AZ31 magnesium alloy,* Surface and Coatings Technology, vol. 236, pp. 52-57, 2013, doi: 10.1016/j.surfcoat.2013.04.059

[20] J. Xu, X. Wang X. Zhu, D. Shan, B. Guo, G. Langdon, *Dry sliding wear of an AZ31 magnesium alloy processed by equal-channel angular pressing*, Journal of Materials Science, vol. 48, iss. 11, pp. 4117–4127, 2013, doi: 10.1007/s10853-013-7224-x

[21] T.S. Yang, G.Z. Chen, *Mechanical Properties and Friction of AZ31 Magnesium Alloy and Application to the Cylidrical Deep Drawing Process*, Key Engineering Materials, vol. 739, pp. 225-230, 2017, doi: 10.4028/www.scientific.net/KEM.739.225

[22] N. Nishioka, L. Chiang, T. Uesugi, Y. Takigawa and K. Higashi. *Dynamic Friction Properties and Microstructural Evolution in AZ31 Magnesium Alloy at Elevated Temperature during Ring Compression Test*, Materials Transactions, vol. 52, iss. 8, pp. 1575-1580, 2011, doi: 10.2320/matertrans.MC201013

[23] J.F. Archard, *Contact and Rubbing of Flat Surface,* Journal of Applied Physics, vol. 24, iss. 8, pp. 981–988, 1953, doi: 10.1063/1.1721448

[24] K. Holmberg, H. Ronkainen, A. Matthews, *Wear Mechanisms of Coated Sliding Surfaces*, Tribology Series, vol. 25, pp. 399-407, 1993, doi: 10.1016/S0167-8922(08)70395-X

[25] A. Da Forno, M. Bestetti, N. Lecis, *Effect of anodising electrolyte on performance of AZ31 and AM60 magnesium alloys microarc anodic oxides,* Journal Transactions of the IMF, vol. 91, iss. 6, pp. 336-341, 2013, doi: 10.1179/0020296713Z.000000000124

[26] A. Němcová, O. Galal, P. Skeldon, I. Kuběna, M. Šmíd, E. Briand, I. Vickridge, J-J. Ganem, H. Habazaki, *Film growth and alloy enrichment during anodizing AZ31 magnesium alloy in fluoride/glycerol electrolytes of a range of water contents,* Electrochimica Acta, vol. 219, pp. 28-37, 2016, doi: 10.1016/ j.electacta.2016.09.089

[27] L. Veleva, M.A. Alpuche-Aviles, M.K. Graves-Brook, D.O. Wipf, *Comparative cyclic voltammetry and surface analysis of passive films grown on stainless steel 316 in concrete pore model solutions,* Journal of Electroanalytical Chemistry, vol. 537, iss. 1-2, pp. 85-93, 2002, doi.org/10.1016/S0022-0728(02)01253-6

[28] E.H.B. Hani, J. Lopez, G. Mohanan, *Data on the coefficient of static friction between surfaces coated with different sizes of rubber granules produced from used tires,* Data in Brief, vol. 22, pp. 940–945, 2019, doi: 10.1016/ j.dib.2019.01.022

[29] W.X. Wang, P. Liu, L.T. Gan, *Research on Friction and Wear Properties of Annealed 5052 Al-Mg Alloy*, Advanced Materials Research, vol. 160-162, pp. 157-162, 2011, doi: 10.4028/www.scientific.net/AMR.160-162.157

[30] L. Giron, W. Aperador, L. Tirado, F. Franco, J.C. Caicedo, *Electrochemical Performance Estimation of Anodized AZ31B Magnesium Alloy as Function of Change in the Current Density,* Journal of Materials Engineering and Performance, vol. 26, iss. 8, pp. 3710–3718, 2017, doi.org/10.1007/s11665-017-2808-2